

Supporting Information

Linkermann et al. 10.1073/pnas.1415518111

SI Materials and Methods

Mice. All WT mice (C57BL/6) reported in this study were obtained from Charles River. Eight- to 12-wk-old male C57BL/6 mice (average weight ~23 g) were used for all WT experiments, unless otherwise specified. Caspase-8 fl/fl mice were kindly provided by Razquella Hakem (Department of Medical Biophysics, University of Toronto, Toronto and Ontario Cancer Institute, University Health Network, Toronto). FADD fl/fl mice were generated by and provided by M.P. Doxycyclin-inducible renal tubule-specific Pax8-rtTA; Tet-on.Cre mice have been published (1) and were kindly provided by Tobias B. Huber (Renal Division, University Medical Center Freiburg, Freiburg, Germany). RIPK3-deficient mice were kindly provided by Vishva M. Dixit. All in vivo experiments were performed according to the Protection of Animals Act, after approval of the German local authorities or the Institutional Animal Care and Use Committee (IACUC) of the University of Michigan, and the National Institutes of Health *Guide for the Care and Use of Laboratory Animals* (2), after approval from the University of Michigan IACUC or by the Local authorities responsible for the approval at Ghent University. In all experiments, mice were carefully matched for age, sex, weight, and genetic background. Genotypes were confirmed by tail-clip PCR using the following primers: Pax8-rtTA forward, 5'-CCATGTC-TAGACTGGACAAGA-3'; Pax8-rtTA reverse, 5'-CTCCAG-GCCACATATGATTAG-3'; tetO-Cre forward, 5'-GCAT-TACCGGTGCGATGCAACGAGTGATGAG-3'; tetO-Cre reverse, 5'-GAGTGAACGAACCTGGTTCGAAATCAGTGCG-3'; caspase-8 flox/flox forward, 5'-ATAATCCCCCAAAT-CCTCGCATC-3'; caspase-8 flox/flox reverse, 5'-GGTCCATCCAGGGGCTTCCT-3'; FADD flox/flox forward, 5'-TCACCGTGTCTTGTGCTAC-3'; FADD flox/flox reverse (I), 5'-GTAATCTCTGTAGGGAGCCCT-3'; and FADD flox/flox reverse (II), 5'-CTAGCGCATAGGATGATCAGA-3'.

Cell Lines and Reagents. Necrostatin (Nec-1) was obtained from Sigma-Aldrich. Sangliferrin A (SfA) was provided by Novartis Pharma. The zVAD-fmk (herein referred to as zVAD) was purchased from BD Biosciences. The monoclonal anti-Fas antibody was from Immunotech. Smac mimetics (Birinapant) was from Absource Diagnostics (Selleckchem). Murine NIH 3T3 fibroblasts were originally obtained from ATCC and were cultured in Dulbecco's modified Eagle medium (DMEM) (Invitrogen) supplemented with 10% (vol/vol) FCS, 100 U/mL penicillin, and 100 µg/mL streptomycin. Human HT-1080 fibrosarcoma cells were originally obtained from ATCC and were cultured in DMEM (Invitrogen) supplemented with MEM NEAA (Invitrogen), 10% (vol/vol) FCS, 100 U/mL penicillin, and 100 µg/mL streptomycin. Murine NIH 3T3 cells were originally obtained from ATCC and were cultured in DMEM (Invitrogen) supplemented with 10% (vol/vol) FCS, 100 U/mL penicillin, and 100 µg/mL streptomycin. Jurkat cells were originally obtained from ATCC and were cultured in RPMI 1640 supplemented with 10% (vol/vol) FCS, 100 U/mL penicillin, and 100 µg/mL streptomycin. All cell lines were cultured in a humidified 5% CO₂ atmosphere.

Induction of Cell Death. For induction of necroptosis, HT-29 cells were stimulated for 24 h at 37 °C with 100 ng/mL TNF α plus 1 µM Smac mimetics plus 25 µM zVAD as indicated (vehicle-treated cells served as control). For induction of ferroptosis, NIH and HT-1080 cells were each stimulated for 24 h at 37 °C with 50 µM erastin as indicated (vehicle-treated cells served as

control). For induction of apoptosis, Jurkat cells were stimulated for 4 h with 100 ng/mL monoclonal anti-Fas (clone 7C11; Immunotech). Anti-Fas-induced apoptosis of Jurkat cells was inhibited by further addition of 25 µM zVAD (vehicle-treated cells served as control).

Analysis of Cell Death. For immunoblotting, cells were lysed in ice-cold 10 mM Tris-HCl, pH7.5, 50 mM NaCl, 1% Triton X-100, 30 mM sodium pyrophosphate, 50 mM NaF, 100 µM Na₃VO₄, 2 µM ZnCl₂, and 1 mM phenylmethylsulfonyl fluoride (modified Frackelton buffer). Insoluble material was removed by centrifugation (14,000 × g, 10 min, 4 °C), and protein concentration was determined using a commercial Bradford assay kit according to the manufacturer's instructions (Bio-Rad).

Equal amounts of protein (17 µg per lane) were resolved on a 12% SDS/PAGE gel and transferred to a nitrocellulose membrane (Amersham Biosciences). Western blot was performed using a polyclonal cleaved caspase-3 antibody (Asp-175 from Cell Signaling) and a corresponding secondary horseradish peroxidase-linked polyclonal anti-rabbit antibody (Acris). Immune complexes were visualized by enhanced chemiluminescence (ECL; Amersham Biosciences).

Fluorescence-Activated Cell Sorting. Phosphatidylserine exposure to the outer cell membrane of apoptotic cells or at the inner plasma membrane of necrotic cells and incorporation of 7-AAD into necrotic cells were quantified by fluorescence-activated cell sorting (FACS) analysis. The ApoAlert annexin V-FITC antibody and the 7-AAD antibody were purchased from BD Biosciences.

Isolation of Renal Tubules. Six to 12 mice were used for each isolated tubule preparation, depending on the amount of material needed for particular experiments. For preparation of isolated tubules, mice were anesthetized with ketamine (100 mg/kg i.p.) and xylazine (10 mg/kg i.p.), and the kidneys were immediately removed. Type I collagenase was from Worthington Biochemical. Percoll was purchased from Amersham Biosciences. All other reagents and chemicals, including delipidated BSA, were of the highest grade available from Sigma-Aldrich. Immediately after removal of the kidneys, the parenchyma was injected with 0.3–0.5 cc of a cold 95% O₂/5% CO₂-gassed solution consisting of 115 mM NaCl, 2.1 mM KCl, 25 mM NaHCO₃, 1.2 mM KH₂PO₄, 2.5 mM CaCl₂, 1.2 mM MgCl₂, 1.2 mM MgSO₄, 25 mM mannitol, 2.5 mg/mL fatty acid-free BSA, 5 mM glucose, 4 mM sodium lactate, 1 mM alanine, and 1 mM sodium butyrate (solution A) with the addition of 1 mg/mL collagenase (type I; Worthington Biochemical). The cortices were then dissected and minced on an ice-cold tile and then resuspended in additional solution A for 8–10 min of digestion at 37 °C, followed by enrichment of proximal tubules using centrifugation on self-forming Percoll gradients. For Nec-1 studies in renal tubules, renal cortices were dissected in ice-cold dissection solution (DS) [HBSS with 10 mmol/L glucose, 5 mmol/L glycine, 1 mmol/L alanine, 15 mmol/L Hepes (pH 7.4); osmolality, 325 mOsmol/L] and sliced into 1-mm pieces. The fragments were transferred to collagenase solution [DS with 0.1% (wt/vol) type 2 collagenase and 96 µg/mL soybean trypsin inhibitor] and digested for 30 min at 37 °C and 61 × g. After digestion, the supernatant was sieved through two nylon sieves: first 250-µm pore size and then 100-µm pore size. The longer proximal tubule segments remaining in the 100-µm sieve were resuspended by flushing the sieve in the reverse direction with warm DS (37 °C) containing BSA 1% (wt/vol). The proximal tubule suspension was

centrifuged for 5 min at $170 \times g$, washed, and then resuspended into the appropriated amount of culture medium (1:1 DMEM/F12 without phenol red and supplemented with heat-inactivated 1% FCS, 15 mmol/L Hepes, 2 mmol/L L-glutamine, 50 nmol/L hydrocortisone, 5 $\mu\text{g}/\text{mL}$ insulin, 5 $\mu\text{g}/\text{mL}$ transferrin, 5 ng/mL sodium selenite, 0.55 mmol/L sodium pyruvate, 10 mL/L 100 \times nonessential amino acids, 100 IU/mL penicillin, and 100 $\mu\text{g}/\text{mL}$ streptomycin buffered to pH 7.4 (osmolality of 325 mOsmol/kg H_2O). The proximal tubule fragments were seeded onto a tissue-culture plate and cultured at 37 °C and 95% air/5% CO_2 in a standard humidified incubator.

Experimental Procedures for, and Movies of, Freshly Isolated Tubules.

Incubation conditions were similar to those used previously for mouse tubule studies (3). Tubules were suspended at 2.0–3.0 mg of tubule protein per milliliter in a 95% air/5% CO_2 -gassed medium containing 110 mM NaCl, 2.6 mM KCl, 25 mM NaHCO_3 , 2.4 mM KH_2PO_4 , 1.25 mM CaCl_2 , 1.2 mM MgCl_2 , 1.2 mM MgSO_4 , 5 mM glucose, 4 mM sodium lactate, 0.3 mM alanine, 5 mM sodium butyrate, 2 mM glycine, and 1.0 mg/mL bovine gelatin (75 bloom) (solution B). For studies comparing normoxia with hypoxia/reoxygenation, at the end of the 15 min, preincubation tubules were resuspended in fresh solution B and regassed with either 95% air/5% CO_2 (normoxic controls) or 95% N_2 /5% CO_2 (hypoxia). During hypoxia, solution B was kept at pH 6.9 to simulate tissue acidosis during ischemia *in vivo*, and the usual substrates (glucose, lactate, alanine, and butyrate) were omitted. After 30 min, samples were removed for analysis. The remaining tubules were pelleted and then resuspended in fresh 95% air/5% CO_2 -gassed, pH 7.4 solution B with experimental agents as needed. Sodium butyrate in solution B was replaced with 2 mM heptanoic acid during reoxygenation and supplemented with 250 μM AMP, 0.5 mg/dL delipidated albumin, and 4 mM each α -ketoglutarate and malate. After 60 min of reoxygenation, tubules were sampled for studies. Movies with perfused isolated tubules recorded in the presence and absence of fatty acids as indicated were taken from C57BL/6 mice, which were killed under deep isoflurane anesthesia by decapitation. Kidneys were removed immediately, sliced, and transferred into incubation buffer (140 mmol/L NaCl, 0.4 mmol/L KH_2PO_4 , 1.6 mmol/L K_2HPO_4 , 1 mmol/L MgSO_4 , 10 mmol/L Na-acetate, 1 mmol/L α -ketoglutarate, 1.3 mmol/L Ca-gluconate, and 5 mmol/L glycine, containing 48 mg/L trypsin inhibitor and 25 mg/L DNase I at pH 7.4). Proximal tubules (PTs) were isolated mechanically and transferred into the bath on a heated microscope stage [Axiovert 10 (PT1) or Axiovert 35M]. Tubules were held by a concentric glass pipette system. The rates of tubular perfusion via the micropipette were 10–20 nL/min. The bath was thermostatted at 37 °C, and continuous bath perfusion at 3–5 mL/min was obtained by gravity perfusion. PTs were monitored by a digital imaging system (Visitron Systems GmbH) and analyzed by MetaFluor software. Brightfield images were obtained every 10–20 s and stored for off-line analysis. Solution I (140 mmol/L NaCl, 0.4 mmol/L KH_2PO_4 , 1.6 mmol/L K_2HPO_4 , 1 mmol/L MgCl_2 , 5 mmol/L glucose, 1.3 mmol/L Ca-gluconate, at pH 7.4) was used for fatty-acid depletion, and Solution II (140 mmol/L NaCl, 0.4 mmol/L KH_2PO_4 , 1.6 mmol/L K_2HPO_4 , 1 mmol/L MgSO_4 , 1.3 mmol/L Ca-gluconate, 10 mmol/L Na-acetate, 1 mmol/L α -ketoglutarate, 5 mmol/L glycine, and 5 mmol/L glucose, at pH 7.4) was used for adapted PT substrate supply.

In Vivo Microscopy on the Postischemic Cremaster Muscle. The surgical preparation of the cremaster muscle was performed as originally described by Baez with minor modifications (1, 4). Mice were anesthetized using a ketamine/xylazine mixture (100 mg/kg ketamine and 10 mg/kg xylazine), administered by i.p. injection. The left femoral artery was cannulated in a retrograde manner for administration of microspheres and drugs. The right cremaster muscle was exposed through a ventral incision of the

scrotum. The muscle was opened ventrally in a relatively avascular zone, using careful electrocautery to stop any bleeding, and spread over the transparent pedestal of a custom-made microscopic stage. Epididymis and testicle were detached from the cremaster muscle and placed into the abdominal cavity. Throughout the procedure as well as after surgical preparation during *in vivo* microscopy, the muscle was superfused with warm-buffered saline.

The setup for *in vivo* microscopy was centered around an Olympus BX 50 upright microscope (Olympus Microscopy), equipped for stroboscopic fluorescence epiillumination microscopy. Light from a 75-W xenon source was narrowed to a near-monochromatic beam of a wavelength of 700 nm by a galvanometric scanner (Polychrome II; TILL Photonics) and directed onto the specimen via an FITC filter cube equipped with dichroic and emission filters (DCLP 500, LP515; Olympus). Microscopy images were obtained with Olympus water immersion lenses [20 \times /numerical aperture (N.A.) 0.5 and 10 \times /N.A. 0.3] and recorded with an analog black-and-white charge-coupled device (CCD) video camera (Cohu 4920; Cohu) and an analog video recorder (AG-7350-E; Panasonic). Oblique illumination was obtained by positioning a mirroring surface (reflector) directly below the specimen and tilting its angle relative to the horizontal plane. The reflector consisted of a round cover glass (thickness, 0.19–0.22 mm; diameter, 11.8 mm), which was coated with aluminum vapor (Freichel) and brought into direct contact with the overlying specimen as described previously (4). For measurement of centerline blood flow velocity, green fluorescent microspheres (2- μm diameter; Molecular Probes) were injected via the femoral artery catheter, and their passage through the vessels of interest was recorded using the FITC filter cube under appropriate stroboscopic illumination (exposure, 1 ms; cycle time, 10 ms; length of the electromagnetic wave, 488 nm), integrating video images for sufficient time (>80 ms) to allow for the recording of several images of the same bead on one frame. Beads that were flowing freely along the centerline of the vessels were used to determine blood-flow velocity.

For off-line analysis of parameters describing the sequential steps of leukocyte extravasation, we used the Cap-Image image analysis software (Dr. Zeintl Biomedical Engineering). Rolling leukocytes were defined as those moving slower than the associated blood flow and were quantified as described previously (4). Firmly adherent cells were determined as those resting in the associated blood flow for more than 30 s and related to the luminal surface per 100- μm vessel length. Transmigrated cells were counted in regions of interest (ROI), covering 75 μm on both sides of a vessel over a 100- μm vessel length. By measuring the distance between several images of one fluorescent bead under stroboscopic illumination, centerline blood-flow velocity was determined. From measured vessel diameters and centerline blood-flow velocity, apparent wall-shear rates were calculated, assuming a parabolic flow-velocity profile over the vessel cross-section.

Animals were treated with ferostatin-1 (2 mg/kg i.p.) or vehicle 30 min before the experiment. For the analysis of postischemic leukocyte responses, three postcapillary vessel segments in a central area of the spread-out cremaster muscle were randomly chosen. After having obtained baseline recordings of leukocyte rolling, firm adhesion, and transmigration in all three vessel segments, ischemia was induced by clamping all supplying vessels at the base of the cremaster muscle using a vascular clamp (Martin). After 30 min of ischemia, the vascular clamp was removed, and reperfusion was restored for 160 min. Measurements were repeated at 60 min and 120 min after onset of reperfusion. Subsequently, FITC dextran was infused intraarterial (i.a.) for the analysis of microvascular permeability. After *in vivo* microscopy, blood samples were collected by cardiac puncture for the determination of systemic leukocyte counts using a Coulter AcT Counter (Coulter). Anesthetized animals were then euthanized by exsanguination.

Analysis of microvascular permeability was performed as described previously (3). Briefly, the macromolecule FITC-dextran (5 mg in 0.1 mL saline, M_r 150,000; Sigma-Aldrich) was infused i.a. after determination of centerline blood-flow velocity. Five postcapillary vessel segments, as well as the surrounding perivascular tissue, were excited at 488 nm, and emission >515 nm was recorded by a CCD camera (Sensicam; PCO) 30 min after injection of FITC-dextran using an appropriate emission filter (LP 515). Mean gray values of fluorescence intensity were measured by digital image analysis (TILLvisION 4.0; TILL Photonics) in six randomly selected ROIs ($50 \times 50 \mu\text{m}^2$), localized 50 μm distant from the postcapillary venule under investigation. The average of mean gray values was calculated.

Acute Oxalate Nephropathy Model. Mice were divided into two groups. One group received vehicle injections and another group received Ferrostatin-1 (10 mg/kg i.p.). Then, 15 min later, both groups were given a single i.p. injection of 100 mg/kg sodium oxalate and 3% sodium oxalate in drinking water. Blood samples and kidneys were harvested after 24 h. Kidneys were kept at -80°C for protein isolation and at -20°C for RNA isolation. One part of the kidney was also kept in formalin to be embedded in paraffin for histological analysis. Kidney sections (2 μm) were stained with periodic acid–Schiff (PAS) reagent. Tubular injury was scored by assessing the percentage of necrotic tubules. Ly6B.2+ neutrophils were identified by immunostaining (clone 7/4; Serotec). Pizzolato stain was used to visualize CaOx crystals, and crystal deposit formation in the kidney was evaluated as described previously (4), using the following point values: 0, no deposits; 1, crystals in papillary tip; 2, crystals in cortical medullary junction; 3, crystals in cortex. When crystals were observed in multiple areas, points were combined. Serum creatinine and blood urea nitrogen were measured using Creatinine FS kit and Urea FS kit (both from DiaSys Diagnostic Systems) according to the manufacturer's protocol. Neutrophil infiltrates were counted in 15 high-power fields (hpf) per section. For real-time quantitative RT-PCR, total RNA was isolated from kidneys using a Qiagen RNA extraction kit following the manufacturer's instructions. After quantification, RNA quality was assessed using agarose gels. From isolated RNA, cDNA was prepared using reverse transcriptase (Superscript II; Invitrogen). Real-time quantitative RT-PCR (TaqMan) was performed using SYBR-Green PCR master mix and analyzed with a Light Cycler 480 (Roche). All gene expression values were normalized using 18S RNA as a housekeeping gene. All primers used for amplification were from Metabion. The expression of KIM-1, IL-6, CXCL-2, and NF- κB p65 was analyzed using the following primers: Kim-1 forward, TCAGCTCGGGAATGCACA; Kim-1 reverse, TGGTTGCCTTCCGTGTCT; IL-6 forward, TGATGCACCTTGCAGAAAACA; IL-6 reverse, ACCAGAGGAAATTTTCAATAG; CXCL-2 forward, TCCAGTCAGTTAGCCTTGC; CXCL-2 reverse, CGGTCAAAAAGTTTGCTTGC; NF- κB p65 forward, CGCTTCTCTCAATCCGGT; NF- κB p65 reverse, GAGTCTCCATGCAGCTACGG.

Kidney Model of Ischemia–Reperfusion Injury. Induction of kidney IRI was performed via a midline abdominal incision and a bilateral renal pedicle clamping for either 40 min (severe IRI, or “lethal-to-WT” IRI) or 50 min (ultra-severe IRI) using microaneurysm clamps (Aesculab). Throughout the surgical procedure, the body temperature was maintained between 36°C and 37°C by continuous monitoring using a temperature-controlled self-regulated heating system (Fine Science Tools). After removal of the clamps, reperfusion of the kidneys was confirmed visually. The abdomen was closed in two layers using standard 6-0 sutures. Sham-operated mice underwent the identical surgical procedures, except that microaneurysm clamps were not applied. To maintain fluid balance, all of the mice were supplemented

with 1 mL of prewarmed PBS administered intraperitoneally directly after surgery. All mice were killed 48 h after reperfusion for each experiment. For assays investigating combination therapy with [Nec-1 + SfA], mice received a total volume of 150 μL of Clinoleic with 10 mg of SfA per kg of body weight and 1.65 mg of Nec-1 per kg body weight 60 min before ischemia. Then, 2 mg of 16-86 or 16-79 per kg body weight were dissolved in 2% DMSO and were applied intraperitoneally as a total volume of 400 μL 15 min before the onset of surgery in all experiments. All ischemia–reperfusion experiments were performed in a double-blinded manner.

Model of Cerulein-Induced Pancreatitis. Cerulein-induced pancreatitis (CIP) has been described elsewhere in detail (3). Briefly, male C57BL/6 WT mice ($n = 7$) and male RIPK3-ko mice ($n = 7$) received i.p. injections of 50 μg cerulein/kg body weight once every hour for 10 h (in each case, 200 μL of total volume supplemented with PBS). Animals were euthanized 24 h after the first injection, and samples of blood and tissues were rapidly harvested. Quantification of pancreas injury was performed by measuring serum amylase and lipase activity.

LPS-Induced Lethal Shock. Mice were injected intraperitoneally (i.p.) with 15 mg/kg *Escherichia coli* O111:B4 LPS (Sigma-Aldrich). Mice were pretreated by an i.p. injection of 5 mg/kg ethyl 3-amino-4-(cyclohexylamino)benzoate (Fer-1; Matrix Scientific), 10 mg/kg [5-((7-Cl-1H-indol-3-yl)methyl)-3-methylimidazolidine-2,4-dione] (Nec-1s; synthesized in house), a combination of Fer-1 and Nec-1s, or vehicle (1% DMSO in PBS) 30 min before the LPS challenge. Rectal body temperature and survival rates were monitored daily up to 96 h. Experiments were approved by the animal ethics committee of Ghent University.

Histology, Immunohistochemistry, and Evaluation of Structural Organ Damage. Organs were dissected as indicated in each experiment and infused with 4% neutral-buffered formaldehyde, fixated for 48 h, dehydrated in a graded ethanol series and xylene, and finally embedded in paraffin. Paraffin sections (3–5 μm) were stained with periodic acid–Schiff (PAS) reagent, according to standard routine protocol. Stained sections were analyzed using an Axio Imager microscope (Zeiss) at 200 \times or 400 \times magnification. Micrographs were digitalized using an AxioCam MRm Rev. 3 FireWire camera and AxioVision ver. 4.5 software (Zeiss). Organ damage was quantified by two experienced pathologists in a double-blind manner on a scale ranging from 0 (unaffected tissue) to 10 (severe organ damage). For the scoring system, tissues were stained with PAS, and the degree of morphological involvement in renal failure was determined using light microscopy. The following parameters were chosen as indicative of morphological damage to the kidney after ischemia–reperfusion injury (IRI): brush border loss, red blood cell extravasation, tubule dilatation, tubule degeneration, tubule necrosis, and tubular cast formation. These parameters were evaluated on a scale of 0–10, which ranged from not present (0), mild (1–4), moderate (5 or 6), severe (7 or 8), to very severe (9 or 10). Each parameter was determined on at least four different animals.

General Procedures for the Synthesis of Ferrostatin-1 and Derivatives.
General Information. Concerning chemicals generally, solvents, inorganic salts, and organic reagents were purchased from commercial sources such as Sigma and Fisher and used without further purification unless otherwise mentioned. For chromatography, Merck precoated 0.25-mm silica plates containing a 254-nm fluorescence indicator were used for analytical TLC. Flash chromatography was performed on 230–400 mesh silica (SiliaFlash P60) from Silicycle. For spectrometry, ^1H , and ^{13}C NMR spectra were obtained on a Bruker DPX 400 MHz spectrometer. High-resolution mass spectrometry (HRMS) spectra

were taken on a double-focusing sector-type mass spectrometer (HX-110A; JEOL Ltd.) [resolution of 10,000 and 10 kV acceleration voltage ionization method, fast atom bombardment (FAB), Xe 3 kV energy, matrix NBA (m-nitrobenzyl alcohol)].

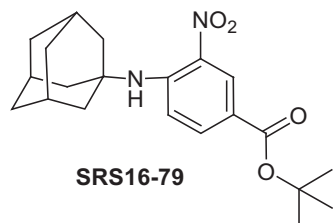
General procedure A (tert-butyl ester formation). To the commercially available 4-chloro-3-nitrobenzoic acid in dichloromethane (1 equiv) was added 4-dimethylaminopyridine (DMAP; 0.3 equiv) and tert-butanol (2 equiv). The *N,N'*-dicyclohexylcarbodiimide (DCC; 1 equiv) was added at 0 °C, and the mixture was stirred for 17 h at room temperature. The precipitate was filtered out under celite, and the organic layer was concentrated under vacuum. The residue was purified by flash-column chromatography on silica gel to provide the desired tert-butyl 4-chloro-3-nitrobenzoate intermediate (Fig. 3A).

General procedure B (ArS_N2 reaction) (5). To the tert-butyl 4-chloro-3-nitrobenzoate intermediate (1 equiv) in dry DMSO (5 mL) was added K₂CO₃ (2 equiv) and 1-adamantylamine (1.2 equiv). The mixture was stirred for 17 h at 60 °C. The solution was poured into water, and the organic layer was extracted three times with ethyl acetate. After drying with anhydrous magnesium sulfate, the solvents were removed under vacuum. The residue was purified by flash-column chromatography on silica gel to provide the desired tert-butyl 4-(adamantyl-amino)-3-nitrobenzoate SRS16-79 (Fig. 3A).

General procedure C (hydrogenolysis). The tert-butyl 4-(adamantyl-amino)-3-nitrobenzoates SRS16-79 (1 equiv) was dissolved in MeOH (10 mL) and hydrogenated (H₂ gas) over 10% Pd(OH)₂ on charcoal (0.1 equiv) for 17 h at room temperature. The solution was filtered through a pad of celite, and volatiles were removed under vacuum. The residue was purified by flash-column chromatography on silica gel to provide the desired tert-butyl 3-amino-4-(adamantyl-amino)benzoate SRS16-82 (Fig. 3A).

General procedure D (imine formation). To the tert-butyl 3-amino-4-(adamantyl-amino)benzoate SRS16-82 (1 equiv) in ethanol (4 mL) and drops of dry HCl 4.0 M in dioxane (10 μL) was added pyrimidine aldehyde (1.1 equiv). The mixture was stirred at 80 °C during 4 h. The solvent was evaporated. The residue was purified by flash-column chromatography on silica gel to provide the desired (*Z*)-tert-butyl 4-(adamantyl-amino)-3-(pyrimidin-5-ylmethyleneamino)benzoate SRS16-86 (Fig. 3A).

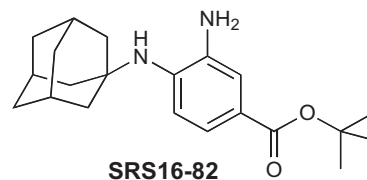
Spectroscopic Characterization.



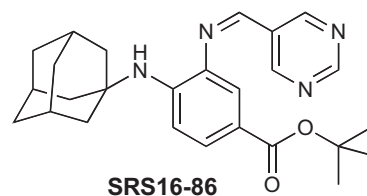
After the above general procedures A and B, the reaction was purified by flash-column chromatography on silica gel to provide

1. Traykova-Brauch M, et al. (2008) An efficient and versatile system for acute and chronic modulation of renal tubular function in transgenic mice. *Nat Med* 14(9):979–984.
2. National Research Council (2011) *Guide for the Care and Use of Laboratory Animals* (National Academies Press, Washington, DC), 8th Ed.
3. Linkermann A, et al. (2012) Dichotomy between RIP1- and RIP3-mediated necroptosis in tumor necrosis factor- α -induced shock. *Mol Med* 18:577–586.

the desired tert-butyl 4-(adamantyl-amino)-3-nitrobenzoate (SRS16-79) (1.08 g, 2.903 mmol, 75%). ¹H NMR (400 MHz, CDCl₃) δ 8.80 (d, *J* = 2.1 Hz, 1H), 8.56 (s, 1H), 7.92 (dd, *J* = 9.2, 2.1 Hz, 1H), 7.19 (d, *J* = 9.2 Hz, 1H), 2.21 (s, 2H), 2.12 (s, 5H), 1.95 (s, 1H), 1.90 (s, 2H), 1.77 (s, 5H), 1.58 (s, 9H); liquid chromatography (LC)/MS (APCI+, *M*+1) 373.03.



After the above general procedure C, the crude reaction mixture was purified by column chromatography (dichloromethane:methanol = 40:1) to provide the desired tert-butyl 3-amino-4-(2-adamantyl-amino)-benzoate (SRS16-82) [700 mg, 2.046 mmol, 88% (3 steps)]. ¹H NMR (400 MHz, CDCl₃) δ 7.47 (dd, *J* = 8.4, 1.9 Hz, 1H), 7.38 (d, *J* = 1.8 Hz, 1H), 6.93 (d, *J* = 8.4 Hz, 1H), 3.33 (s, 2H), 2.15 (s, 3H), 1.99 (s, 6H), 1.72 (s, 6H), 1.57 (s, 9H); LC/MS (APCI+, *M*+1) 343.09.



After the above general procedure D, the reaction was purified by flash-column chromatography on silica gel to provide the desired tert-butyl 4-(adamantyl-amino)-3-(pyrimidin-5-ylmethyleneamino)benzoate (SRS16-86) (200 mg, 0.462 mmol, 89%). ¹H NMR (400 MHz, CDCl₃) δ 9.30 (s, 10H), 9.29–9.15 (m, 33H), 8.66 (d, *J* = 4.1 Hz, 14H), 7.99–7.70 (m, 28H), 7.19–6.92 (m, 14H), 5.58 (s, 13H), 2.13 (d, *J* = 46.0 Hz, 117H), 2.00 (s, 21H), 1.75 (s, 106H), 1.71–1.54 (m, 140H); low-resolution mass spectrometry (FAB+, *M*+) 432.1; HRMS (FAB+) calculated for C₁₆H₂₄N₂O₂: 432.2525; found: 432.2541.

Statistics. For all experiments, differences of datasets were considered statistically significant when *P* values were lower than 0.05, if not otherwise specified. Statistical comparisons were performed using the two-tailed Student *t* test. Asterisks are used in the figures to specify statistical significance (**P* < 0.05; ***P* < 0.02; ****P* < 0.001). *P* values in survival experiments (Kaplan–Meier plots) were calculated using GraphPad Prism Version 5.04 software. Statistics are indicated as SD (not to SEM).

4. Mulay SR, et al. (2013) Calcium oxalate crystals induce renal inflammation by NLRP3-mediated IL-1 β secretion. *J Clin Invest* 123(1):236–246.
5. Beaulieu PL, et al. (2006) Improved replicon cellular activity of non-nucleoside allosteric inhibitors of HCV NS5B polymerase: From benzimidazole to indole scaffolds. *Bioorg Med Chem Lett* 16(19):4987–4993.

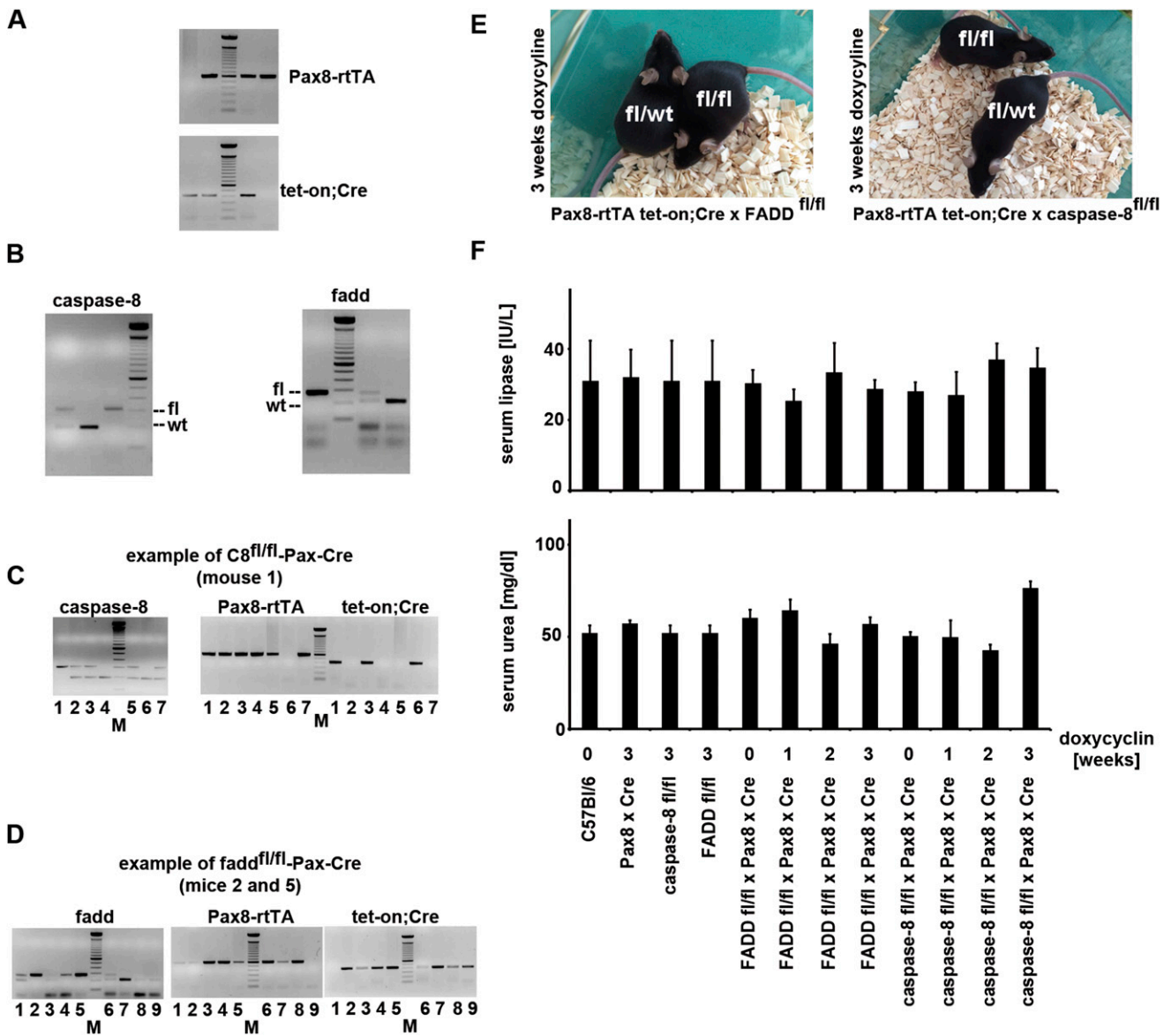


Fig. S1. Generation of doxycyclin-inducible kidney tubular specific conditional FADD- and caspase-8 knockout mice. (A–D) Representative genotyping of either FADD-inducible or caspase-8 doxycyclin-inducible kidney tubular-specific conditional knockout mice. (E) Indistinguishability of fl/wt and fl/fl mice after doxycyclin treatment for 3 wk via the drinking water (see *Materials and Methods* for details). (F) Mice of the indicated genotypes were treated for 0 wk, 1 wk, 2 wk, or 3 wk with doxycyclin before detection of serum lipase (*Upper*) and serum urea (*Lower*) levels ($n = 3-8$ per group for all blood values).

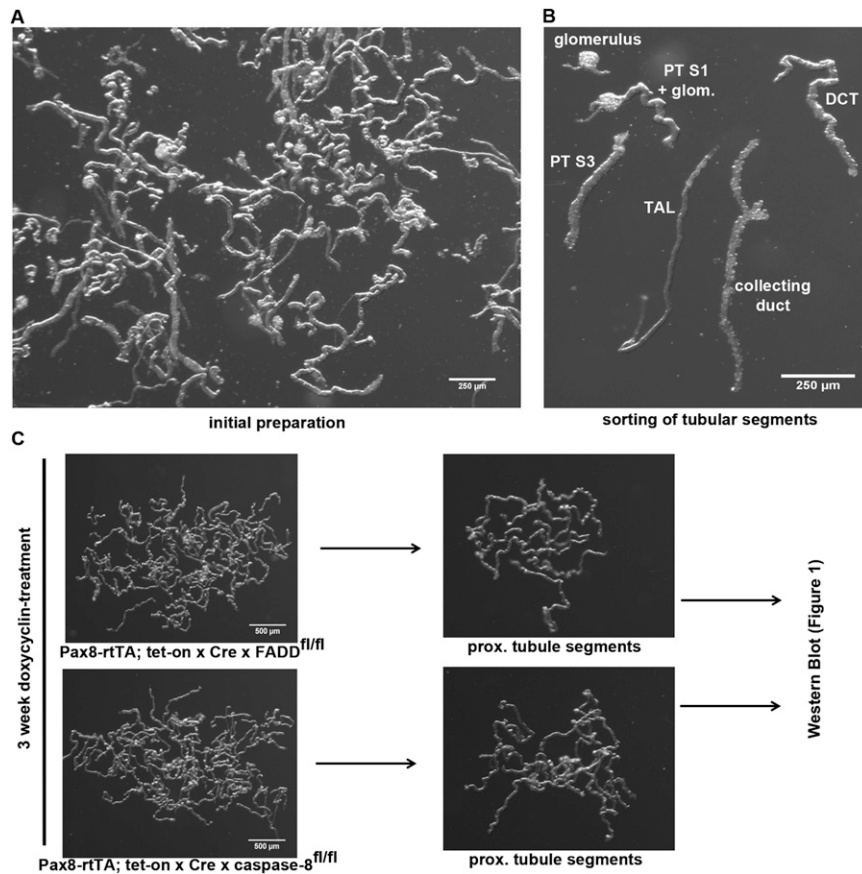


Fig. S2. Preparation of murine renal tubules for Western blot analysis and microperfusion movies. (A) Classical appearance after performance of the initial enzymatic preparation steps (see *Materials and Methods* for details). (B) Overview of hand-picked tubular segments. For Western blot analysis, proximal tubules were collected due to the very high susceptibility to undergo necrosis in acute kidney injury. (C) Doxycyclin-fed mice were killed after 3 wk of transactivator induction, and renal tubules were collected. Proximal tubular segments were subsequently pooled and loaded onto gels for Western blotting in Fig. 1. DCT, distal convoluted tubule; TAL, thick ascending limb.

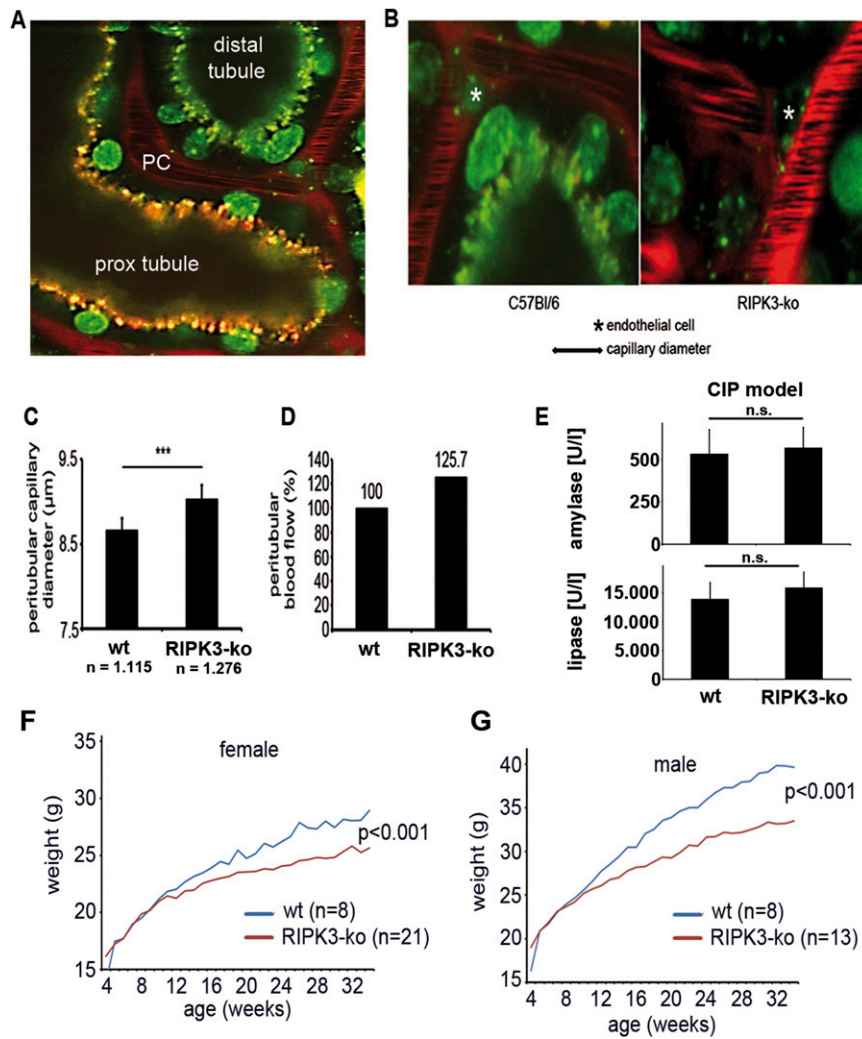


Fig. 53. RIPK3-deficient mice have a phenotype. (A) Example of high-resolution intravital microscopy. Green, autofluorescence of the kidney tubules; red, 70 kDa rhodamine dextran (applied via a jugular catheter); yellow, Texas Red (2 kDa) dye, which is freely filtered in the glomerular and reabsorbed in the proximal tubule, counterstaining the endolysosomal compartment; PC, peritubular capillary. For a dynamic impression on how this endolysosomal compartment works, compare Movie S2. (B and C) Intravital microscopy reveals significantly increased peritubular diameters in untreated RIPK3-deficient mice compared with WT littermates. Data in C were generated by counting the diameters of peritubular capillaries at a number of at least 1.115 per group. (D) Based on the data presented in B, the increase in peritubular diameters is associated with 125.7% overall organ perfusion in RIPK3-deficient mice. (E) Model of cerulein-induced pancreatitis (CIP) in WT and RIPK3-deficient mice. No significant protection from increased serum concentrations of serum lipase or serum amylase was detected in RIPK3-deficient mice compared with WT mice ($n = 7$ mice per group). (F and G) Failure to gain overall body weight in both female (Left) and male (Right) RIPK3-deficient mice compared with corresponding littermates, followed for 30 wk after an age of 4 wk ($n = 8$ –21 per group).

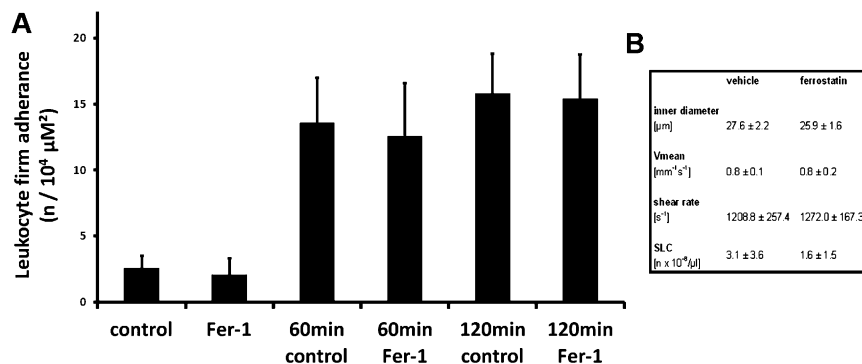


Fig. 54. Leukocyte adherence remains unchanged in IRI of the cremaster muscle upon addition of Fer-1. (A) Intravital evaluation of intravascular firm adhesion of leukocytes in postcapillary venules following 1 h and 2 h after onset of reperfusion. (B) Measurement of microhemodynamic parameters and systemic leukocyte counts, as indicated, based on intravital microscopy in the presence and absence of Fer-1.

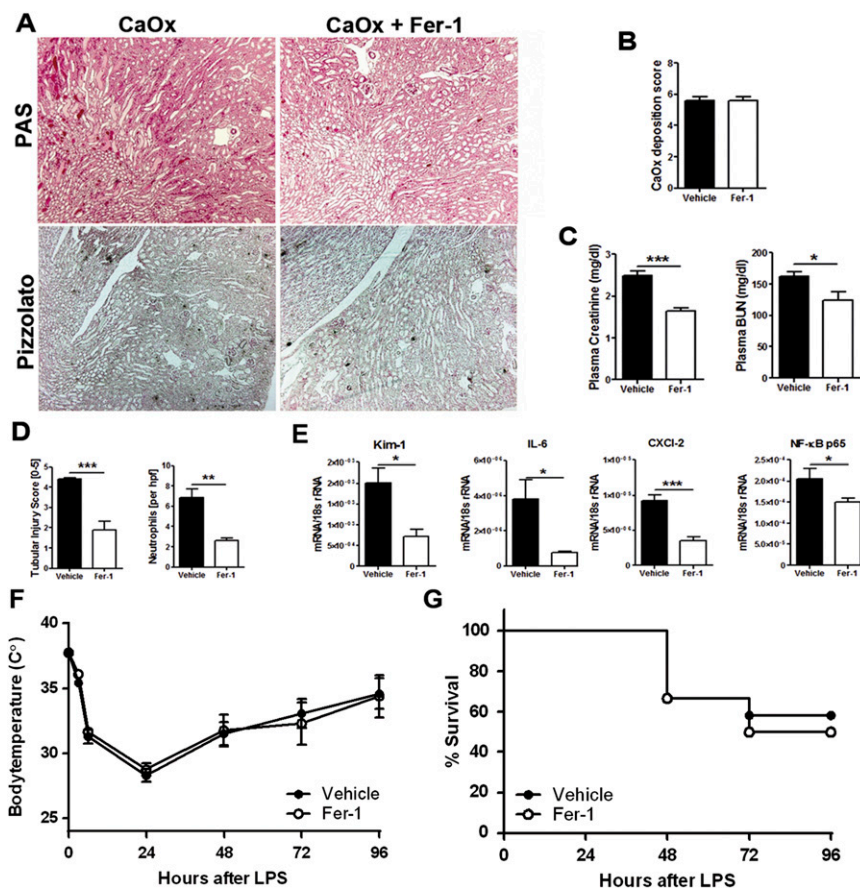


Fig. S5. Ferroptosis contributes to crystal-induced acute kidney injury, but not to the LPS-induced shock model. (A) PAS and Pizzolato staining of mice treated with CaOx and Fer-1. (B) CaOx deposition is not different between the two groups. (C) Evaluation of functional markers of acute kidney injury in mice that underwent CaOx-induced nephropathy. (D) Fer-1 significantly reduces the ultrastructural damage in CaOx nephropathy. (E) Significant reduction of expression of Kim-1 (TIM-1), IL-6, CXCL2, and p65 in the Fer-1-treated Ca-Ox model (* $P = 0.05$ – 0.02 , ** $P = 0.02$ – 0.001 , *** $P \leq 0.001$; $n = 8$ – 10 per group). (F and G) In the model of LPS-induced septic shock, 12 mice per group were injected intraperitoneally with LPS as described in *SI Materials and Methods*. (F) Temperature drop and (G) overall survival rates following 96 h after LPS injection ($n = 12$ per group, error bars indicate SEM).

Table S1. Microsomal stability of SRS15-72A in mouse

Test compound	Elimination rate		Intrinsic clearance (CL _{int}), mL/min per g liver
	constant (k)	Half-life ($t_{1/2}$), min	
SRS15-72A	0.3419	2.0	35.90
Ethoxycoumarin	0.1591	4.4	16.71

Microsomal stability (mouse, compound concentration = $0.5 \mu\text{M}$). Microsomal stability and intrinsic clearances of SRS15-72A in hepatic microsomes. Ethoxycoumarin was used as a control compound. Half life more than 90 min was reported as >90 , and less than 1.4 was reported as <1.4 . Rate constants for microsomes less than 0.0048 or negative were reported as <0.0048 , and more than 0.48 were reported as >0.48 .

Table S2. Microsomal stability of SRS15-72A in mouse

Test compound	Elimination rate		Intrinsic clearance (CL _{int}), mL/min per g liver
	constant (k)	Half-life ($t_{1/2}$), min	
SRS15-72A	0.0045	154.0	0.47
Ethoxycoumarin	0.1885	3.7	19.79

Microsomal stability (mouse, compound concentration = $0.5 \mu\text{M}$). Microsomal stability and intrinsic clearances of SRS15-72A in hepatic microsomes. Ethoxycoumarin was used as a control compound. Half life more than 90 min was reported as >90 , and less than 1.4 was reported as <1.4 . Rate constants for microsomes less than 0.0048 or negative were reported as <0.0048 , and more than 0.48 were reported as >0.48 .

Table S3. Stability of SRS15-72A and SRS15-72B in mouse plasma (strain C57BL/4)

Compound name	Parent (<i>m/z</i>)	Time point, min	Condition			
			Room temperature		Wet ice	
			Peak area ratio	% remaining	Peak area ratio	% remaining
SRS15-72A	405	0	2.0737	100.0	2.6066	100.0
SRS15-72A	405	15	1.1581	55.8	2.0815	79.9
SRS15-72A	405	30	0.5320	25.7	1.6279	62.5
SRS15-72A	405	60	0.2502	12.1	1.4397	55.2
SRS15-72A	405	120	0.0841	4.1	1.2446	47.7
SRS15-72B	407	0	5.8556	100.0	6.9233	100.0
SRS15-72B	407	15	0.6709	11.5	5.7631	83.2
SRS15-72B	407	30	0.0885	1.5	4.7595	68.7
SRS15-72B	407	60	0.0206	0.4	3.4547	49.9
SRS15-72B	407	120	0.0159	0.3	1.9564	28.3

Percent remaining, percentage of peak area at each time point compared with peak area at 0 min.

Table S4. Stability of SRS16-80 and SRS16-86 in mouse plasma (strain C57BL/6)

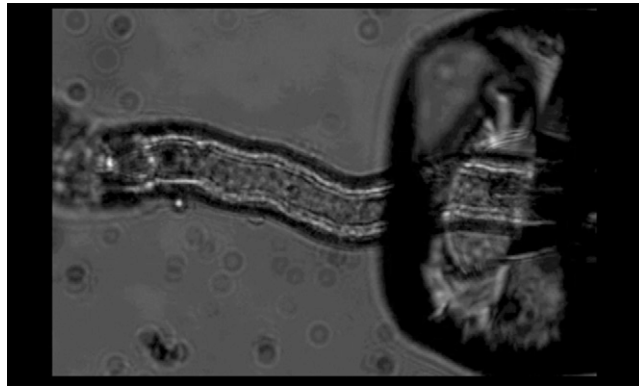
Compound name	Parent (<i>m/z</i>)	Time point, min	Sum of peak	% remaining
SRS16-80	419.2	0	0.3820	100.0
SRS16-80	419.2	15	0.0911	23.8
SRS16-80	419.2	30	0.0379	9.9
SRS16-80	419.2	60	0.0170	4.5
SRS16-80	419.2	120	0.0095	2.5
SRS16-86	433.6	0	0.9018	100.0
SRS16-86	433.6	15	0.7414	82.2
SRS16-86	433.6	30	0.7800	86.5
SRS16-86	433.6	60	0.7568	83.9
SRS16-86	433.6	120	0.5758	63.9

Temperature, 37 °C. Percent remaining, percentage of peak area at each time point compared with peak area at 0 min.

Table S5. Microsomal stability of SRS16-80 and SRS16-86 in mouse

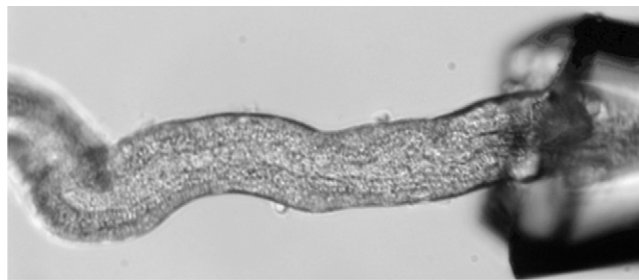
Test compound	Elimination rate constant (<i>k</i>)	Half-life ($t_{1/2}$), min	Intrinsic clearance (CL _{int}), mL/min per g liver
SRS16-80	0.0089	77.7	0.94
SRS16-86	-0.0032	-213.7	-0.34
Ethoxycoumarin	0.2661	2.6	27.94

Microsomal stability (mouse, compound concentration = 0.5 μM). Microsomal stability and intrinsic clearances of SRS16-80 and SRS16-86 in hepatic microsomes. Ethoxycoumarin was used as a control compound. Half life more than 90 min was reported as >90, and less than 1.4 was reported as <1.4. Rate constants for microsomes less than 0.0048 or negative were reported as <0.0048, and more than 0.48 were reported as >0.48.



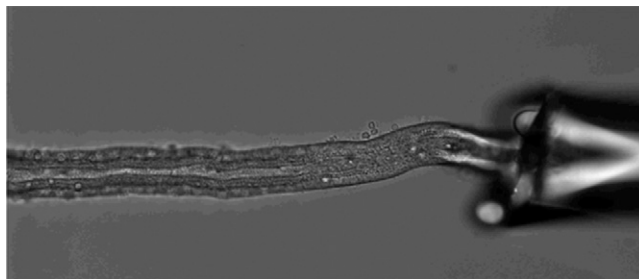
Movie S1. Synchronized tubular necrosis. Dynamics of synchronized tubular necrosis upon depletion of fatty acids (see *Materials and Methods* for details). Note that the synchronized event occurs secondarily after initial necrosis of individual cells. The overall appearance after the synchronized necrotic event morphologically very much resembles casts in urine sediments of patients with acute tubular necrosis (ATN), the classical diagnosis of acute kidney injury (AKI).

[Movie S1](#)



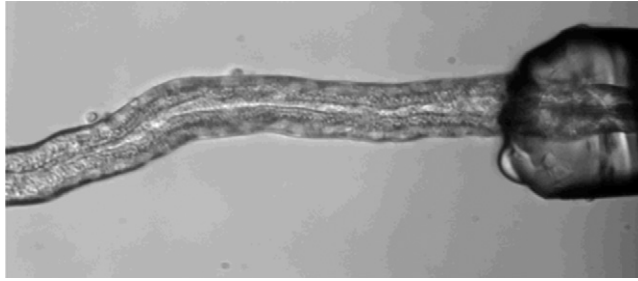
Movie S2. High-resolution movie and quality control of the functional endolysosomal compartment in freshly isolated renal proximal tubules. In the presence of fatty acids, synchronized necrosis does not spontaneously occur within the first hour of video monitoring. These preparations were used for all subsequent tubule experiments.

[Movie S2](#)



Movie S3. Erastin application induces synchronized tubular necrosis. In the presence of fatty acids, synchronized necrosis occurs within minutes [full movies range from 1 to 20 min (Movie S3) and 1–30 min (Movie S4 in higher resolution) after erastin addition to the perfusion solution]. Movies S3 and S4 represent two examples of this event in completely independent settings.

[Movie S3](#)



Movie S4. Erastin application induces synchronized tubular necrosis. In the presence of fatty acids, synchronized necrosis occurs within minutes [full movies range from 1 to 20 min (Movie S3) and 1–30 min (Movie S4 in higher resolution) after erastin addition to the perfusion solution]. Movies S3 and S4 represent two examples of this event in completely independent settings.

[Movie S4](#)